GOCE RADAR-BASED ORBIT DETERMINATION FOR RE-ENTRY PREDICTIONS AND COMPARISON WITH GPS-BASED POD

S. Cicalò[(1)], J. Beck[(2)], E. Minisci[(3)],
F. Guerra[(1)], I. Holbrough[(2)], S. Lemmens[(4)], A. Riccardi[(3)], and M. Vasile[(3)]

[(1)]*Space Dynamics Services S.r.l., via Mario Giuntini 63, 56023 Navacchio di Cascina (PI), Italy, Email: cicalo@spacedys.com*
[(2)]*Belstead Research Ltd, 387 Sandyhurst Lane, Ashford, Kent, UK*
[(3)]*Department of Mechanical & Aerospace Engineering, University of Strathclyde, James Weir Building, 75 Montrose Street, Glasgow, G1 1XJ, UK*
[(4)]*ESA/ESOC Space Debris Office (OPS-GR), Robert-Bosch-Str. 5, 64293 Darmstadt, Germany*

ABSTRACT

During the last days of its re-entry phase, GOCE was tracked by several on-ground and in-orbit instruments, mainly radar and GPS. The availability of such a rich data set at low altitudes provides a unique opportunity to gain insight in the field of re-entry analysis. This study aims at understanding if general re-entry prediction strategies can be improved, especially from the point of view of orbit determination techniques. Precise orbits from continuous GPS measurements are compared with orbits determined from single- and simulated multi-sensor radar measurements. The conclusion is that, provided a proper observational frequency, even sparse radar tracking can give comparable information to continuous on-board GPS solutions, if the goals are re-entry predictions and average ballistic coefficient estimation. At low altitudes, large intrinsic uncertainties in the dynamical models dominate over the observational errors, affecting orbit precision, measurement residuals and limiting predictions accuracy. For this reason, to guarantee observational sessions up to few hours before re-entry is always recommended to reduce the size of re-entry windows.

Key words: GOCE; re-entry; POD; radar; ballistic coefficient.

1. INTRODUCTION

During its three weeks of uncontrolled re-entry phase, the Gravity field and steady-state Ocean Circulation Explorer (GOCE) satellite was tracked by several on-ground sensors and in-orbit instruments, mainly radar and GPS, and the acquired data was analyzed by several teams. The data was processed both directly and in Two-Line Element (TLE) format, to generate re-entry predictions ([4], [5]). Due to the peculiar nature of the spacecraft, and of its attitude controller, the re-entry campaign proved to be quite unusual, with different attitude behaviors to consider. The large uncertainties in the physical limits of the controller dominated the final uncertainties in the re-entry predictions, leaving the Orbit Determination (OD) problems in the background. Dedicated works are present in the literature, focused on the TIRA sensor of the Fraunhofer institute for High Frequency Physics and Radar Techniques, and on GPS-based Precise Orbit Determination (POD) ([2], [3]). The conclusion was that, provided a proper observational strategy, the single site tracking gives comparable information to on-board GPS solutions, if the goal is re-entry predictions.

In order to better understand this counter-intuitive result, SpaceDyS has employed its Software capable of performing GPS-based POD, radar-based OD and simulations of radar observations. Here we mainly focus on radar-based OD performances, aiming at assessing the dependency of the re-entry prediction uncertainties, and ballistic coefficient estimation, on the quality of the OD and of the observational features. We make only general considerations about the choice of a particular atmospheric density model, the predictability of space weather events, or independent techniques for attitude estimation.

First of all, we exploit the large amount of GPS and attitude measurements to compute a POD during the last weeks of GOCE re-entry, this is described in Section 2. The POD orbital states can be used later for orbit comparison and for accurate extrapolation of the ballistic coefficient evolution. Then, in Section 3 we discuss the use of the TIRA measurements to compute standard OD and ballistic coefficient estimation for re-entry predictions. The corresponding extrapolation made only with radar measurements is studied in depth, making also use of a radar-data simulator, described in Section 4, which can generate artificial observations from further ground stations, using the POD as ground truth.

A direct comparison between the ballistic coefficient calibration obtained with the GPS and the radar observations, respectively, is given in Section 5. Particular attention

Proc. 7th European Conference on Space Debris, Darmstadt, Germany, 18–21 April 2017, published by the ESA Space Debris Office
Ed. T. Flohrer & F. Schmitz, (http://spacedebris2017.sdo.esoc.esa.int, June 2017)

will be paid in considering both single-sensor and multi-sensor scenarios.

Finally, an attempt to generalize the results obtained for GOCE to similar simulated orbits for objects of different shapes (spherical or cylindrical) is discussed in Section 6.

2. GPS-BASED PRECISE ORBIT DETERMINATION

2.1. Overview

The GOCE spacecraft was equipped with a GPS LAGRANGE receiver that provided accurate data (at the level of a few centimeters of post-fit RMS of the GPS un-differenced carrier phase residuals). In addition to the GPS data, attitude measurements, Satellite Laser Ranging (SLR) and radar data were acquired during the operational lifetime of the mission and during the re-entry phase. Thanks to this dense dataset, the POD of the spacecraft up to the very last moments of its life can be performed, exploiting different computational techniques.

The GPS receivers provide phase measurements which can be processed to provide the spacecraft positions. Different methods and techniques can be exploited to perform this POD stage. To obtain the best results the processing is usually performed with a reduced dynamics method (e.g. [7]): the orbit of the spacecraft is determined only over a short arc, under a dynamical model including empirical accelerations to be solved simultaneously. The empirical accelerations absorb both the non-gravitational perturbations and the inaccuracies in the knowledge of the gravitational accelerations. This process has been shown to be accurate to a few cm in all directions in the spacecraft position over the entire mission [1]. In the generation of the GOCE Precise Science Orbit (PSO) three constant acceleration parameters were estimated, over an entire orbital arc of 30h, and 6-min piece-wise constant accelerations in radial, along-track, and out-of-plane directions, with the same constraints for the entire mission. This procedure has two important implications: first, the common mode data from the on-board accelerometers (i.e., the components of the gradiometer) do not need to be used in the POD; second, the GPS data do not provide useful information on the gravity field, because the empirical acceleration mix together the gravitational signal with the non-gravitational one. Note that, even though the common-mode accelerations from the GOCE gradiometer are not used for the reduced-dynamics POD, these data proved to be useful in improving the reduced-dynamic orbit determination results by deriving realistic constraints for the empirical accelerations [1]. Moreover, although the empirical accelerations absorb most of the un-modeled perturbations, the adoption of state-of-the-art dynamical models both for the gravitational and non-gravitational perturbations is able to further improve the quality of the solution.

The other most commonly used POD technique is the so-called kinematic method. In the kinematic orbit computation the position of GOCE is computed separately for each epoch using GPS data at only that epoch. Consecutive GOCE position estimates are made independent from each other, apart from possible correlations that might exist in supporting data, e.g. orbit errors in the GPS ephemeris that have predominantly a 12-hour correlation time. The kinematic POD is possible because of the strong GPS observing geometry. The quality of the position estimate at each epoch will vary with changing observing geometry in combination with instantaneous errors like measurement noise, atmospheric correction errors, and GPS ephemeris errors. Also, the changing effect of ground station coordinate errors (each epoch has a different geometry of ground stations) will show up directly in the GOCE satellite position estimates. A disadvantage of this approach may be the strong non-homogeneity of the quality of the position estimates due to changing observation geometry and changing measurement errors. Also, at times of data outages no GOCE position estimates can be made.

In this study, the POD task will be performed using the SpaceDyS's software GREOD (GOCE Re-Entry Orbit Determination), with support from Belstead Research Ltd. (BRL) for the aerodynamics perturbations models. The proven high accuracy orbit generation techniques will be implemented and validated by a comparison with already published results, in particular the ones presented in [2] and [1].

2.2. Observational and dynamical model

The baseline POD for the production of the required reference orbit is performed with a reduced dynamics method [8], following the same dynamical and observational assumptions of the reference literature [2] and [1] as close as possible. This allows us for a more reliable validation of the results.

The observation data set to be processed by the fit consists of about 21 days of continuous, un-differenced, GPS code and carrier-phase dual-frequency measurements. Due to the high accuracy of these observations, precise information on the position of the GPS antenna is also required, in terms of Center of Mounting Plane with respect to the satellite Center of Mass, antenna Phase Center Offsets (PCOs) and Phase Center Variations (PCVs). Thus, also the attitude states measured by the on-board Star Trackers are necessary. All this material has been provided to SpaceDyS (SDS) by ESA, as CFI of the EXPRO+ "Benchmarking re-entry prediction uncertainties" project.

Besides clock synchronization corrections and carrier-phase biases, a suitable number of empirical local parameters is determined for each orbital arc, to account for the un-modeled part of the perturbations. The latter consists of along- and cross-track Cycle Per Revolution

(CPR, see [9]) accelerations every 1h, plus one drag scaling coefficient every 15 minutes. Nonetheless, state-of-the-art dynamical models for the gravitational and non-gravitational perturbations are adopted to improve the quality of the solution and gain insight into the physical parameters driving the orbital evolution. In particular, luni-solar third body perturbations, indirect oblation, General Relativity corrections, a GOCE-derived gravity field (EIGEN-6C 200×200) for the gravitational perturbations, along with suitable solid and oceanic tides models (IERS2003, FES2004).

As regards the non-gravitational perturbations, we consider only a standard drag acceleration computation of the form:

$$\mathbf{a}_{drag} = -\frac{1}{2} C_d \frac{A}{m} \rho v_r^2 \hat{\mathbf{v}}_r \tag{1}$$

where A is the reference area of the spacecraft, C_d is the drag coefficient, m is the satellite mass, ρ is the atmospheric density at the spacecraft location (e.g. modeled by NRLMSISE00), $\hat{\mathbf{v}}_r$ is the direction of the relative velocity of the spacecraft with respect to the atmosphere and $v_r = |\mathbf{v}_r|$. For the relative velocity computation, we assume that the atmosphere is rotating fixed with the Earth [9]. The mass during the re-entry phase is about 1000kg. Variations of the ballistic coefficient $C_d A/m$ due to attitude motion have been suitably implemented by means of an aerodynamic database, provided by BRL, in function of the yaw angle (see Figure 1), which is the dominant term in the GOCE attitude motion, and of the speed ratio of the spacecraft.

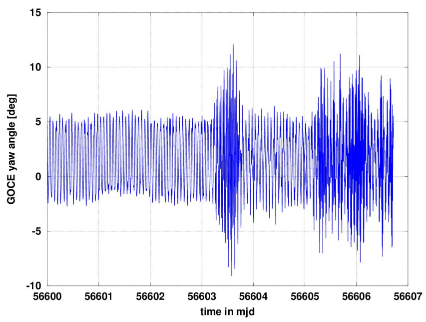

Figure 1. GOCE yaw angle behavior during the last week of re-entry (from attitude measurements [2]).

2.3. POD results

Each single day of re-entry has been processed independently from the others, solving for the initial conditions of the spacecraft, the empirical acceleration parameters, the clock corrections and carrier-phase biases, for a total of thousands of parameters to be determined per day.

The results for the POD computation obtained with GREOD, following the same approach of [2], have been compared directly not only with the explicit results presented in the paper, but also with the corresponding solution for the orbital states, provided to us by ESA and that we called Reference Re-Entry Orbits (RREO). Another term of comparison is the Precise Science Orbit (PSO), computed by the Astronomical Institute of the University of Bern (AIUB), with slightly different dynamical assumptions, available for the first 16 days of re-entry and for the entire drag-free phase of the GOCE mission. The validation for the reliability of our POD procedures mainly consisted in direct comparisons between the empirical parameters solutions, the orbital states differences, and the observations residuals, both during the 21 days of re-entry in 2013 and during days of drag-free phase in 2009 and 2010. To describe in detail all these results in this paper is not possible, but we can claim that the procedures were considered successful within the development of the project.

In general, the post-fit RMS of the un-differenced carrier-phases exponentially grow from less than 1cm during the first week to about 10cm during the last days of re-entry, which are more or less in line with [2, Fig.8]. The explicit 3D orbit difference RMS with respect the reduced-dynamic PSO and the RREO solutions are shown in Figure 2.

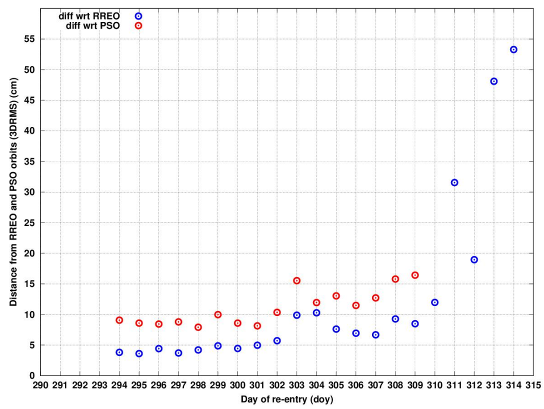

Figure 2. 3D orbit difference RMS with respect the reduced-dynamic PSO and the RREO solutions.

During the last 4 days of re-entry, where the aerodynamic forces grow up by orders of magnitude, the 3D-RMS difference with respect to the RREO orbits grows up to ∼0.5m. The main problem in computing a precise and accurate orbit is to reconstruct the dynamical un-modeled or not well modeled terms, which grow significantly at low altitudes. Better empirical acceleration models are possible, which give smaller residuals and, most probably, also a smaller uncertainty in the orbit determination. Due to the high accuracy of the available GPS measurements, and the generally accepted levels of accuracy of GPS-based POD, we believe that an accuracy level of few meters is not questionable here, even for the last day. The differences with respect to PSO and RREO are always well below the m-level. On the contrary, a specific dedicated analysis to demonstrate lower, few-dm level orbit determination during the last week of re-entry would require, for example, independent sources of information, and they will not be considered here.

However, the main issue of this study is the analysis of re-entry prediction uncertainties, while the standard uncertainties in the orbit determination of an object during re-entry, e.g. with radar observations, are much larger than the ones of the special case of GOCE under continuous GPS tracking. For this reason, we believe that the POD obtained can effectively be used as reference orbit for the next part of the work without any loss of accuracy.

2.4. GPS-based PWC ballistic coefficient estimation

Let us focus on the last days of POD available, in which we have a dense measurements data set. We know from previous results that, if we want to reproduce the dynamics of GOCE during its last days of POD at sub-meter level of accuracy, we need a complex overparametrization of the unknown portion of dynamics. A reconstruction of the physical meaning of these un-modeled perturbations is a tough problem, and it is not straightforward how to use them for the purpose of future re-entry predictions.

In preparation for the analysis of radar-based calibration of re-entry predictions, and in particular of the estimation of the ballistic coefficient to be used for re-entry propagations, we can further exploit the POD orbital states. We can actually use the orbital states as an ideal, continous, set of observations, from which we can extrapolate a refined behavior of the ballistic coefficient. The $C_d A$ drag (or ballistic) coefficient (the mass m is considered well known in this case) can be modeled as a piece-wise constant (PWC) function, in order to capture its short-term variations. Depending on the length of each constant we can obtain different levels of accuracy.

Short term variations due to attitude motion and atmospheric density errors can not be captured by sparse radar tracking measurements, thus we need to find a trade-off value for this analysis. We can see in Figure 3 an example of fit with a 10-min, 30-min and 3-hours PWC drag coefficient. The atmospheric density model adopted is NRLMSISE00. The $C_d A$ variations need to absorb errors in the atmosperic density model and the attitude motion (mainly yaw motion). Since, in this case, the attitude motion has a period close to 90-min, the larger oscillations of the 10-min PWC show this effect, while the 3-hours PWC shows mainly the average drag variations. The 30-min PWC shows instead short-term variations at the order of 10-20% of the mean value, compatible with the expected error level in the atmospheric density models [10]. The 10-min and 30-min PWC estimations lead to orbit accuracies (i.e. differences with respect to POD) below the 10m-level during the entire last week of re-entry, while the 3-hours PWC is worse by at least an order of magnitude.

This results anyway in an accurate estimation of the drag coefficient behavior over the time span covered by GPS measurements. In Figure 4 the result for the 30-min PWC drag coefficient estimation is shown, with the three different atmospheric density models: NRLMSISE00, Jacchia-Bowman 2008, and Jacchia-Roberts static. Note that the qualitative behavior of the function does not depend on the particular choice of the atmospheric density model, which is also analogous to the accurate estimation of the GOCE C_d from the ESA Flight Dynamics team, discussed in [4, Fig.6]. Again, also the particular mean values assumed by the function in the same sub-intervals can differ by even 10-20%, as a direct consequence of the nominal differences in the density models themselves. We have reported in Figure 5 the values of the corresponding estimated, un-modeled, perturbative acceleration (along-track), very useful to understand the radar-based OD results.

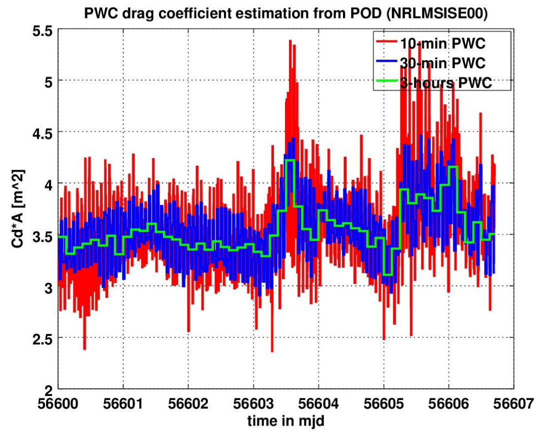

Figure 3. PWC $C_d A$ [m^2] coefficient estimation from POD, with 10-min (red), 30-min (blue), and 3-hours constant time intervals (green). NRLMSISE00 atmospheric density model is adopted.

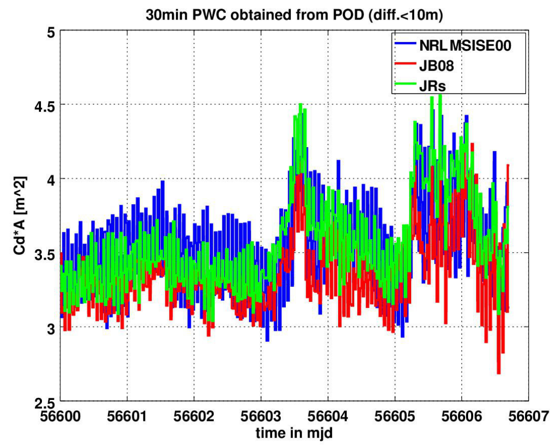

Figure 4. 30min-PWC $C_d A$ [m^2] coefficient estimation from POD, with different atmospheric density models.

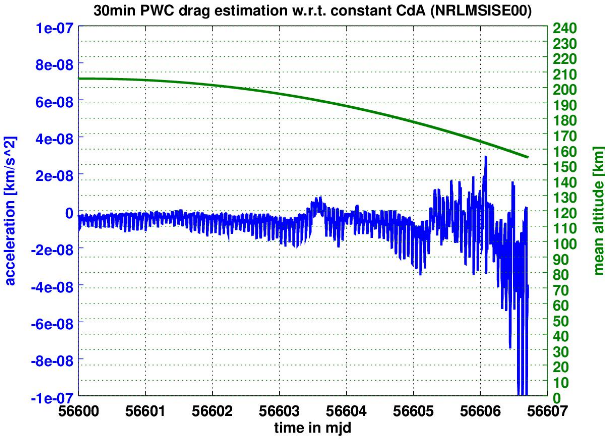

Figure 5. Corresponding estimated (along-track) 30min-PWC drag acceleration correction with respect to a nominal model with constant $C_d A \cong 3.9\ m^2$ (mean value on mjd-56605, day Nov-9).

3. RADAR-BASED ORBIT DETERMINATION AND RE-ENTRY PREDICTIONS

3.1. TIRA tracking passes

A set of tracking passes, taken during the GOCE re-entry phase by the TIRA station, has been provided to SDS by ESA, as CFI of the project, along with the set of corresponding solutions for the orbital states and drag coefficient determination obtained in the fits discussed in [3].

The data consists of 12 tracking passes of about 5 minutes each, taken in October and November 2013, until ~17 hours before the actual re-entry, see [3, Tab.1]. In that work, it was attempted to derive, for combinations of multiple passes among all the 12, the following quantities:

- 6 initial conditions of the GOCE spacecraft at an epoch close to the last pass;
- one drag scaling coefficient.

At the end, a total of 15 fits were accepted to be used for re-entry predictions. They are summarized in [3, Tab.2].

In general, what happens is that for combinations of two or three passes over less than two days it is possible to obtain residuals of the order of decameters in range and centi-degrees in azimuth and elevation. While for combinations of four or more passes over more than two days the residuals grow up by at least one order of magnitude. Another effective term of comparison is the global difference (3D-RMS) with respect to the POD, which, in the best cases, is at the order of hectometers in radial, kilometers in along-track and decameters in cross-track directions.

This is likely due to the fact that the estimation of a single drag scaling coefficient is not enough to absorb the significant mis-modelings in the drag perturbations, which grow with the altitude decrease. Errors in the atmospheric environment model, and in the spacecraft's average attitude, at low altitudes produce errors in the orbit that are much larger than the ~10m in range and ~0.01° in azimuth/elevation TIRA level of accuracy. This can be seen both from the comparison with the POD, and also when we fit the last four passes together.

A dense parametrization of empirical accelerations is necessary to reproduce the POD, and this is possible if the measurements are not only accurate, but also continuous. This is not the case for radar-based observations. For a low polar orbiter like GOCE, the visibility conditions are quite strict, and, depending also on the site latitude, it is possible to observe the spacecraft only for few minutes every 10-14h.

We reproduced the same computations presented in [3], also in order to validate our radar-based orbit determination processes. In general, we obtained an acceptably good agreement with the corresponding results presented in the paper, at least for the orders of magnitude.

Let us focus for instance on fit no. 13 and 12 of [3], which are about the best and the worse fit available among all the 15, respectively. The weights of the observation passes are usually set at the same order of magnitude of the expected measurement's noise. For TIRA measurements, which is considered an highly capable tracking sensor, we used as nominal values 10m for range and 0.01° for azimuth and elevation (RMS values). As discussed before, due to large systematic errors in the dynamical models, it is not possible to have neither small residuals everywhere nor small differences with respect to the POD everywhere, and it happens that the weights are not always consistent with the actual residuals RMS values after the fit. This is extremely evident in fit no.12. The comparison of the main results, obtained with a uniform data weight of the different passes, are gathered in Table 1. A more detailed comparison would have required more information and details on all the assumptions and settings adopted in [3], in particular for the exact parametrization used for solar flux F10.7 and space weather Kp variations at the time of the experiment.

Table 1. Results of observations fit no. 13 and 12 of [3], comparison with GREOD (NRLMSISE00).

fit no.	Range RMS[km]	Az. RMS[°]	Elev. RMS[°]	$C_d A$ [m^2]
13 [3]	0.052	0.009	0.030	4.0479
13 GREOD	0.024	0.010	0.016	3.8568
12 [3]	0.751	0.032	0.116	3.9578
12 GREOD	0.453	0.034	0.139	3.7606

3.2. Calibration of re-entry predictions

Standard re-entry predictions procedures usually consider the last available information on the spacecraft's state, e.g. last TLE or last radar-based data, to be the starting point for its re-entry propagation in the future and for the calibration of its drag (ballistic) coefficient in the past (see [11], [12]). For instance, the preliminary analysis given in the previous subsection seems to indicate that, in the case of GOCE, predictions performed in the morning of Nov-10 are difficult to calibrate. In order to understand more in depth this kind of problems, and provide indications on good radar observation strategies, we will focus on the following steps: (i.) use of the POD to extrapolate more accurate information on drag coefficient variations (previous Subsection 2.4); (ii.) use of the POD to simulate radar tracking passes from more ground stations, to test possible improvements in the drag coefficient calibration (next Section 4); (iii.) assessments on maximum information obtainable from realistic radar-based measurements and comparison between single-sensor (i.e. TIRA only), multi-sensor and GPS-based performances for re-entry predictions.

3.3. Considerations on Orbit Determination uncertainties

It is not straightforward to extract and associate an uncertainty to the orbit determination performed with more tracking passes, in the presence of significant un-modeled systematic errors in the dynamics. The assumption of estimating a constant drag coefficient implies that GOCE is approximated by a sphere-like object, which is not, and the atmospheric density models are likely affected by significant errors. This fact is quite clear from all the results of [3], especially when we directly compare the radar-based fitted orbits with the GPS-based reference orbit. The estimation of a constant ballistic coefficient is not capable to absorb all the un-modeled drag effects. Figures 4 and 5 give us a quantitative idea of the missing component of drag force that we need to take into account to keep the orbit uncertainty small.

If large systematic errors are not properly taken into account in the orbit determination least squares fit, the covariance matrix will not be reliable, giving small uncertainties compared to the true errors [9]. As an example, in Table 2 the difference between the radar-based fitted orbit and the POD reference orbit is compared, at the initial epoch, with the formal covariance (STD) associated to the same quantities. These values are not coherent because the formal covariance contains only the information on the measurements noise but not on the significant dynamical errors.

As discussed in [14], the strategy of "consider parameters" seems to be appropriate to overcome this problem, where the dominant error source is the atmospheric drag $\mathbf{a}_{drag}$. In that work, it is proposed to include the effects due to drag modeling errors by a correction factor

Table 2. Formal covariance for initial position and difference w.r.t. the POD at in.cond. epoch Nov-10∼7:30 UTC.

fit no.	formal STD RTW[m]	diff. w.r.t. POD RTW[m]
13	∼(0.9, 0.6, 0.5)	∼(87.0, 9.1, 60.0)
12	∼(0.6, 0.4, 0.5)	∼(1142.0, 152.0, 308.0)

$\mathbf{a}_{drag} \to (1+\delta)\mathbf{a}_{drag}$, where δ is a PWC function, or the sum of more functions, which plays the role of consider parameters. Its noise is modeled as a (stationary Gauss-Markov) stochastic process with properties:

$$E[\delta_i] = 0\,,\ E[\delta_i \delta_j] = \sigma^2 e^{-|i-j|\alpha}\,, \qquad (2)$$

where E is the expectation operator, δ_i is the value of δ for each interval of time τ, σ^2 is the variance and α is related to the correlation time of the process (see also [13]). The particular choice of τ, σ and α would require a dedicated analysis, based on the real POD results and on the state of the art atmospheric density error models. We are not going to perform such a specific analysis here, leaving this to possible future activities. However, we would like to perform a very preliminary attempt in this direction, based on quite general considerations, to see how the Table 2 results could change.

Following [9], if we indicate with x the 7-dimensional vector of solve for parameters (6-dim state vector + 1-drag coefficient), with B_x the partial derivatives of the measurements residuals with respect to x, and with W the weight matrix of the observations, then the formal covariance matrix associated to the least squares fit solution is $\Gamma = (B_x^T W B_x)^{-1}$. If the consider parameters c are assumed to be small random quantities with zero mean and covariance Γ_c, uncorrelated with the measurement noise, then the covariance matrix that includes also the consider effects on the solve for parameters estimation is:

$$\Gamma_x^c = \Gamma + (\Gamma B_x^T W)(B_c \Gamma_c B_c^T)(W B_x \Gamma)\,, \qquad (3)$$

where B_c are the partial derivatives of the measurements residuals with respect to c.

A very preliminary attempt can be made by exploiting the results obtained in Subsection 2.4, where the un-modeled behavior of the drag coefficient $C_D A$ is estimated from POD as a PWC function, including effects due to atmospheric density errors. A possible test value for τ is 30-min, while a quite conservative uncertainty variance can be set to 10% of the nominal value, i.e. $\sigma = 0.1$. The choice of the correlation parameter α would also need a suitable justification. We chose as a test value $\alpha = 0.35$, implying a correlation between subsequent parameters to vanish in a couple of satellite's orbits.

The corresponding consider covariance results are given in Table 3, showing a much better agreement with the true errors. In this respect, the POD could be exploited in more and more depth to find other, better, configurations, for the consider parameters assumptions. With this

Table 3. Formal covariance, with consider parameters, for initial position and difference w.r.t. the POD at in.cond. epoch Nov-10∼7:30 UTC.

fit no.	formal STD RTW[m]	diff. w.r.t. POD RTW[m]
13	∼(97.4, 16.5, 59.8)	∼(87.0, 9.1, 60.0)
12	∼(1577.0, 218.0, 158.0)	∼(1142.0, 152.0, 308.0)

preliminary representation of the formal covariance, we have also a formal uncertainty quantification for the ballistic coefficient estimation. The corresponding formal uncertainties for fit no. 13 and 12 are about 3.9% and 3.1%, respectively (in percentage of the nominal value). We can note an improvement, likely due to the larger time span of fit no.12, but at the price of a worsening in the initial conditions uncertainty shown in Table 3. We believe it cannot be considered a significant improvement. On the contrary, there could be an intrinsic limit in the improvements reacheable by adding more observations, because of the large uncertainties in the dynamical models.

4. SIMULATED SCENARIOS

The main purpose of this Section is to understand if and how different observational scenarios could improve the quality of the orbit determination and consequently reduce the uncertainty of re-entry predictions. Following the preliminary analysis given in Section 3, we will make use of the GREOD radar-simulator in order to generate possible different scenarios of GOCE observations from multiple stations. Among these different scenarios we will attempt to individuate the main features that are important for a good orbit determination.

The derived reference orbit POD of GOCE described in Section 2, will be used as ground truth until Nov-10 ∼17:20 UTC. For completeness, a nominal reference orbit is used to check for visibility conditions up to re-entry on Nov-11 ∼00:16 UTC.

4.1. Selection of ground stations and visibility conditions

One of the most important feature that affects visibility conditions from a ground radar station to a low polar orbiter, such as GOCE, is the station's latitude. In principle, higher latitudes allow for more visibility. In order to have a quite complete representation of various latitudes and longitudes, that can guarantee a good frequency of tracking passes, we will follow [6], and choose the six stations given in Table 4. Another feature allowing for more real-

Table 4. Ground stations considered for simulations (are hypothetical sites).*

	Station	latitude	longitude
1	TIRA, Germany	∼51°	∼7°
2	Kiruna, Sweden	∼68°	∼20°
3	Kourou, French Guiana	∼6°	∼307°
4	New Zeland	∼-40°	∼175°
5	North-West Russia*	∼67°	∼40°
6	Center Russia*	∼57°	∼80°

istic scenarios is the noise associated to each station. In our case, only TIRA is considered at high accuracy level ∼10m in range and ∼0.01° in azimuth/elevation, while the others are at conventional accuracy level ∼30m in range and ∼0.03° in azimuth/elevation. These values are used as standard deviations to generate the corresponding random noise (Gaussian Normal Distribution with zero mean) in the simulation of the observables, and to weigh the data. In the generation of the tracking passes we consider the spacecraft as "visible" only if its elevation is above 2°, a sampling rate of 1Hz is assumed. A further selection can be performed by discarding passes with a too low elevation peak (<10°), even though, in critical situations, all the data available could be useful in principle. No addition of tropospheric refraction effects is considered in the simulations, assuming that they are already removed to a level lower than the considered noise (see e.g. [9]). A deeper dedicated analysis on this latter topic is considered beyond the purposes of this work.

If we focus on the last days of re-entry, from Nov-7 to Nov-10 2013, the results for the simulated GOCE tracking passes from the six ground stations considered can be summarized as in Figure 6. The typical length of each tracking pass is few minutes, while the maximum elevation peak can vary significantly from one pass to another. A representative example of the characteristics of the radar tracking passes is given in [3, Tab.1].

As we can deduce from Figure 6, if we define an observational scenario as a "realistic" subset of passes among all the simulated ones, we have a very large number of possibilities. What we want to investigate here, is in which extent a multi-sensor setup could improve the orbit determination and drag estimation, and the consequent re-entry predictions.

Before defining the procedures that we will use to analyze these problems, we note that many insightful information can be already deduced from the literature [6], [3], and from the results presented in Section 3:

- typical length of good passes is few minutes, ele-

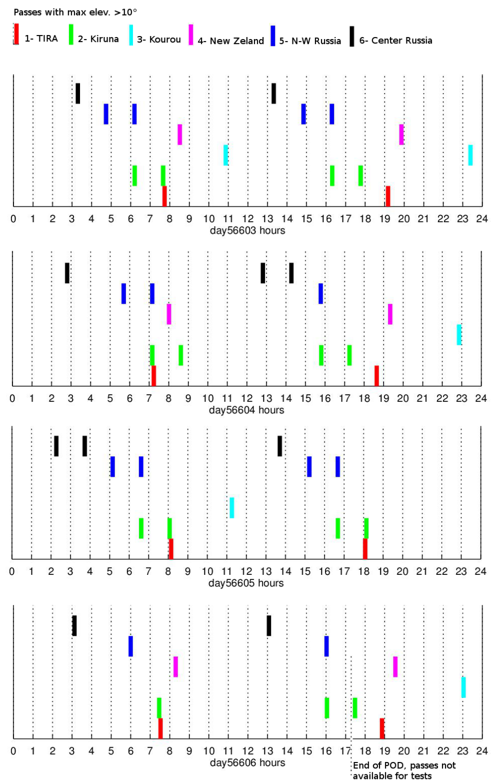

Figure 6. Graphical representation of visibility conditions from the six ground stations considered. Only passes with maximum elevation peaks $> 10°$ are kept. Typical length of passes is few minutes (from ∼250s to ∼350s).

vation peaks can be quite low, so there is very little margin in the choice of elevation cut-off or arc's length;

- passes with higher elevation peak and lower minimum range carry on more information;
- to observe both ascending and descending passes is better;
- passes very close in time are not enough to estimate an average drag coefficient;
- passes too distant in time could be more difficult to fit with a single drag coefficient;
- stations with higher latitude offer more visibility conditions for a polar orbiter;
- multiple stations must be distributed at different longitudes to have more frequent tracking passes during a day;
- a single-station scenario like the TIRA one proved itself to be good enough for standard re-entry predictions requirements.

From now on we will focus only on simulated radar tracking.

4.2. Re-Entry prediction scenarios

In this section we want to test how a multi-sensor scenario would help in improving a re-entry prediction by using a standard approach. We will keep as basic scenarios the fits no.13-12 like of Table 1, with epoch of prediction fixed on Nov-10∼7:30am. With the same philosophy of [3, Tab.2], and the definition of observational scenario given before, we would like to consider all the possible scenarios from Figure 6 with the last TIRA pass in common (the one at ∼7:30). Each of them represents a possible standard calibration of the GOCE ballistic coefficient for the same re-entry prediction. Since the range of possibilities is huge, and moreover, having so many passes all available is certainly a non-realistic assumption, we decided to adopt a specific optimization technique to explore the different cases. For this purpose, in collaboration with University of Strathclyde, we have developed a program which exploits the Open Source software for optimization *Dakota* (Parallel Framework for Optimization and Uncertainty Quantification) and GREOD.

Fixed an epoch of prediction, the optimization program explores among the scenarios obtained with multiple ground stations with suitable constraints on the total number of passes and with a suitable objective function. At this state of knowledge, we believe that a good radar-based solution should be an orbit which stays close to the true one as much as possible. Since we have the POD available for comparison, which corresponds to the ground truth, we can define as objective function a quantification of the difference between the two orbits over the total observation time span, such as the 3D-RMS of the differences in position (e.g. one state every 60s of POD). As regards the total number of passes allowed by the procedure, we fixed a maximum number of 7, covering a period of maximum 36h in the past from the morning of Nov-10. The Dakota exploration of possible scenarios converged after about one thousand cases, toward a solution with a total of only 5 passes. This result, along with the corresponding re-entry predictions and the comparison with the TIRA-only solutions, is shown in Table 5.

Even if it is not possible to prove that the solution provided by Dakota is unique, and there can exist similar but different ones, it is clear that the process discarded the scenarios which cover a large time span (∼36h), converging to a "fit no.13-like" solution (i.e. TIRA last 3 passes) that covers a ∼24h time span. Moreover, even if the addition of tracking passes from other stations improved the solution in terms of difference with respect to the POD, the drag coefficient calibration and the consequent re-entry predictions are equivalent. Another important thing to note is that the multi-sensor solution shows a much larger value of range residuals with respect to the TIRA last 3 passes solution. This was anticipated in Section 3, when we discussed that, during the considered time span, the average differences with respect to the POD were much larger than the 10m-level of accuracy, and that this could have emerged if we fit many passes together. It is evident from Table 5 that it is not straight-

Table 5. Examples of standard re-entry predictions of GOCE based on different selections of passes, all computed ∼17h before actual re-entry to a nominal altitude of 90km (NRLMSISE00). The multi-sensor solution consists of a selection of 5 passes over ∼24h from Kiruna (2 passes on Nov-9 at ∼8:00 and ∼16:30), TIRA (2 passes on Nov-9 at ∼18:00 and Nov-10 at ∼7:30, and New Zeland (1 pass on Nov-10 at ∼8:30).

Adopted passes	tot. obs. time span	Diff. w.r.t. POD [km] (3D-RMS)	Range res. [km] (RMS)	Estim. $C_d A$ [m^2]	re-entry time (mm/dd∼hh:mi) UTC
multi-sensor 5p.	∼24h	∼0.374	∼0.137	3.8555	11/10∼22:13
TIRA-last 3p.	∼24h	∼0.420	∼0.016	3.8561	11/10∼22:13
TIRA-last 2p.	∼12h	∼1.060	∼0.010	3.7859	11/10∼22:40
TIRA-last 4p.	∼36h	∼3.123	∼0.435	3.7605	11/10∼22:51
TIRA-last 5p.	∼48h	∼6.558	∼5.352	3.6764	11/10∼23:23

forward to distinguish which aspects of the re-entry predictions are due to problems in the modeling of the dynamics, and which ones to the particular choice of observational strategy. However, we will see in the following that it is possible to understand in more depth this problem, by the more extensive exploitation of the POD for the ballistic coefficient estimation given in Section 2.4.

5. RADAR-BASED VS GPS-BASED BALLISTIC COEFFICIENT CALIBRATION

So far we have considered a "good radar-based solution" one with a small total difference with respect to the POD, but we can also argue from Figure 4 that a good solution is also one with a drag coefficient that well represents the average value of the GPS-based PWC function. The average value has to be considered meaningful over the limited total observation time span available, hence, depending on the particular functional form of the PWC in that interval, we can try to foresee what we can expect from a good OD:

- there is an evident correlation between the behavior of the GPS-based PWC drag coefficient and the variations of the GOCE yaw angle (see Figure 1);
- with same drag coefficient variations, depending on the nominal altitude of the spacecraft, we have different variations in the magnitude of the corresponding perturbative acceleration (Figure 5);
- the variations of the missing perturbative acceleration on days Nov-8 (mjd-56604), Nov-9 and Nov-10 are significantly large, thus it will be more difficult to fit data covering all days (e.g. ∼36h of TIRA last 4 passes);
- as we get closer to re-entry, the variations of the missing perturbative acceleration become larger and larger (up to ∼15-20% of the nominal value), then, if we fit an orbit with a single drag coefficient, we will obtain large variations with respect to the POD (confirmed by Table 5);
- it may be possible to fit many passes (>3) together with a single drag coefficient, but it may be very difficult to obtain small residuals for each pass (see again Table 5);
- it is not obvious to state a-priori which time interval to consider to calibrate the drag coefficient correctly, besides the fact that it can be actually difficult to state which one is the most correct for future predictions (see also [11]).

5.1. TIRA-only radar-based ballistic coefficient calibration

We know from Figure 6 that the TIRA last available pass for tests is the one on Nov-10, at ∼7:30, since the subsequent visible pass at ∼18:45 was neither available as CFI, nor possible to simulate because the POD ends at ∼17:20. Thus, starting from the evening of Nov-7, we would be able to provide at least six re-entry prediction, one every 10-14 hours. By the lesson learned in Subsection 4.2, we know that there are some difficulties in estimating an average drag coefficient from too distant passes. However, a very naive frequency analysis of the signal showed in Figure 4 suggests that, on the one hand, we will never be able to estimate the short-term 30-min oscillations with sparse radar tracking, while, on the other hand, that an observational frequency of ∼12-24h could be quite effective in reproducing the longer-term average variations. The algorithm we propose is then to fit all the sets of 2 and 3 subsequent TIRA passes to perform the re-entry predictions. The main results are gathered in Table 6 and Figure 7, they confirm that the seven TIRA passes can be suitably exploited to estimate the average behavior of the drag coefficient very effectively, in comparison with the more accurate behavior deduced from the huge amount of information given by the POD, i.e. by continuous GPS measurements.

Table 6. Predictions from TIRA passes, each obtained by fitting only 2-3 consecutive passes distant ∼12-24h. True re-entry time is nominally assumed t_{re}^{tr}=Nov-11-00:16UTC. All the epochs are in November 2013 and in UTC.

pred.#	# of passes	prediction epoch t_0	reentry time t_{re} (at 90km)	$C_D A$[m^2]	reentry error $\frac{t_{re}-t_{re}^{tr}}{t_{re}-t_0}$[%]
1	2	11/7∼19:14	11/10∼20:23	3.8002	∼-5.3%
2	2	11/8∼07:18	11/10∼23:48	3.6251	∼-0.7%
3	2	11/8∼18:40	11/11∼01:44	3.5195	∼2.7%
4	2	11/9∼08:11	11/11∼03:26	3.4120	∼7.3%
5	2	11/9∼18:04	11/10∼22:17	3.8432	∼-7.0%
6	2	11/10∼07:30	11/10∼22:40	3.7859	∼-10.5%
7	3	11/8∼07:18	11/10∼22:24	3.7003	∼-2.9%
8	3	11/8∼18:40	11/11∼00:23	3.6001	∼0.2%
9	3	11/9∼08:11	11/11∼2:54	3.4453	∼6.2%
10	3	11/9∼18:04	11/10∼23:45	3.6810	∼-1.7%
11	3	11/10∼07:30	11/10∼22:13	3.8561	∼-13.9%

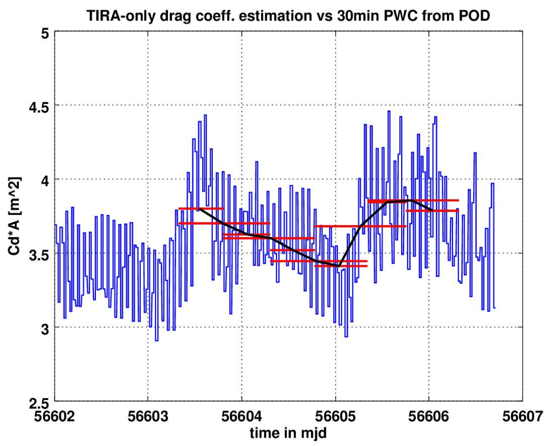

Figure 7. In red, the drag coefficients estimated from the sets of 2-3 subsequent TIRA passes, superposed to the blue 30min PWC drag coefficient function obtained from POD. The black line shows the behavior of the drag coefficient obtained with TIRA-only tracking. Each red line covers the corresponding scenario's observation time span.

A number of interesting issues can be deduced by these results, and by a comparison with Subsection 4.2. As a matter of fact, scenarios which share the same prediction epoch, i.e. the same last pass, can be compared together as in Table 5. The conclusion is straightforward, when we try to fit the last four passes together we obtain a drag coefficient which averages also the long-term variations of the un-modeled perturbative acceleration (Figure 5), at the price of large residuals and large differences with respect to the POD. This large variation can be seen both from predictions no.4 and 5 of Table 6. On the contrary, when we try to fit the last three passes we do not have the same large variation, and the problem is much less evident. In general, on equal values of ballistic coefficient, the more the altitude decreases the more the absolute value of the corresponding un-modeled perturbative acceleration increases. Thus, it will always be more difficult to fit multiple radar tracking passes with the same accuracies, as the spacecraft approaches the re-entry.

It is interesting to note at this point that, in principle, it is possible to fit together even more than 4 subsequent passes, if we properly balance the preliminary data weights. A solution fitting all the last 5 passes (i.e. ∼48h) exists, the problem is that it will never satisfy the accuracy level of the TIRA measurements, and thus the fit will be difficult to converge. However, if we perform a preliminary data deweighing of passes, with ∼5km in range, and ∼0.5° in azimuth and elevation, the fit converges and we obtain the solution of Table 5.

A specific discussion must be dedicated to the corresponding errors in the re-entry times shown in Table 6. As it is commonly done in reentry prediction analysis, the expected re-entry time error $t_{re} - t_{re}^{tr}$ is compared to the re-entry time interval $t_{re} - t_0$, where t_{re} is the predicted re-entry time, t_0 is the epoch of prediction, and t_{re}^{tr} is the actual re-entry time (which is assumed to be on Nov-11-00:16UTC for GOCE). An empirical proportional error of 20% is typically expected (uniform probability). Nominally, all the errors shown in Table 6 are well below the 20% threshold level, but the uncertainty in these values should take into account at least a contribution from the uncertainty in the initial conditions and drag coefficient estimation, which are on their own affected by the intrinsic errors in the atmospheric density models and attitude, and in the forecast of the drag perturbation in between the epoch of prediction and the epoch of actual re-entry. Note that if we apply the consider parameters assumptions as introduced in Subsection 3.3, for each prediction given in Table 6 we obtain a corresponding 1σ formal uncertainty in the drag coefficient estimation of about 3-4% for scenarios with 3 passes, and 4-5% for scenarios with 2 passes.

5.2. Multi-sensor radar-based ballistic coefficient calibration

We obviously believe that the availability of more than one ground station is always preferable, simply because we can obtain a larger amount of information, and that some stations must be always needed as backup in case of malfunctioning of the nominal one. This problem must be analyzed from at least three points of view: (i.) frequency of re-entry predictions, (ii.) ballistic coefficient estimation, (iii.) optimization of resources.

With a single ground station it is not guaranteed to have a tracking pass available few hours before re-entry. In the case of GOCE and TIRA, the last possible tracking pass was around Nov-10$\sim$18:45, i.e. about 5 hours before actual re-entry, however this pass was not recorded by the radar and the only pass available on Nov-10 is the one at $\sim$7:30 in the morning. For different polar orbiters the last pass could be between $\sim$10h before and right before re-entry. For example, it is stated in [5] that a re-entry prediction issued $\sim$4 hours before re-entry is good enough also for civil protection activities.

We have learned in the previous Subsection 5.1 that subsequent radar passes distant $\sim$12-24h can be exploited for a quite acceptable reconstruction of the drag coefficient's unknown behavior during the last 4 days of re-entry. With all the six ground stations considered we have a much higher frequency of passes, this means that, in principle, the average behavior of the drag coefficient could be determined more accurately.

To decide how to combine the passes in order to have an optimal estimation of the drag behavior could be a quite demanding work, also because we should analyze the situation at different nominal altitudes. Here we want to give an idea of the possible different estimation we can perform with more stations during the last days of the GOCE re-entry, with the following cases: A) TIRA and Center Russia stations available; B) all the six stations available.

Case B) gives a very high, not realistic, frequency of passes, about one every orbit. Case A) allows for a $\sim$6-10h frequency of passes, quite balanced. All the scenarios are generated with the condition of at least a $\sim$3h time span covered by the measurements, with at least 3 passes. The corresponding results are graphically shown in Figure 8 and 9, and confirm both that with more passes the average behavior is better captured, and the fact that with TIRA-only tracking the result is anyway very good.

However, the problem of lack of data, and thus of predictions, during the last $\sim$12h of re-entry with TIRA station only available cannot be solved without considering an additional station. A trade-off solution with the addition of just one, polar and well separated in longitude station seems to be fairly acceptable. Anyway, it is worth noting that such a conclusion certainly needs to be tested in more depth, also in different frameworks with different orbiters, e.g. not polars or in more elliptic orbits.

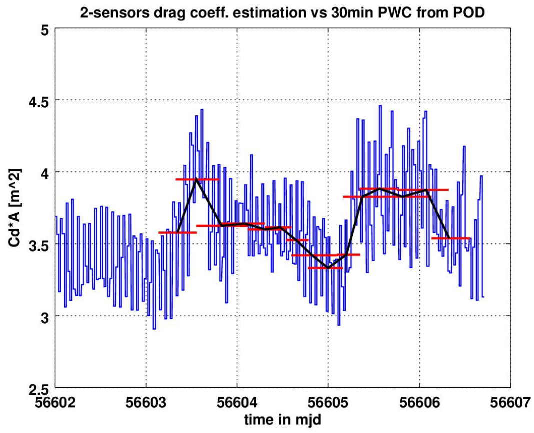

Figure 8. In red, the drag coefficients estimated from scenarios of >2 subsequent TIRA + Center Russia station passes, superposed to the blue 30min PWC drag coefficient function obtained from POD. In black the radar-based average behavior.

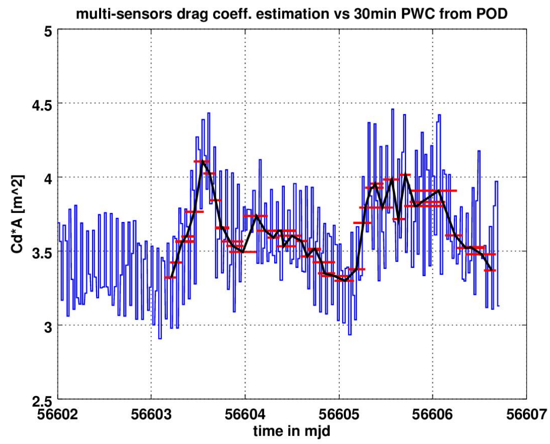

Figure 9. In red, the drag coefficients estimated from scenarios of >2 subsequent passes from all the six stations considered, covering at least 3h, superposed to the blue 30min PWC drag coefficient function obtained from POD. In black the radar-based average behavior.

6. POSSIBLE GENERALIZATIONS

Whether the shorter-terms that appear in Figures 3 and 4 are mainly due to errors in the atmospheric density model, to smaller attitude variations, or to a combination of the two, is something that needs a specific analysis. Some aspects have already been discussed in Subsection 2.4.

We present here two preliminary tests, which are based on the same philosophy of the study described so far for the GOCE case. We want to introduce two different objects placed in the same orbit of GOCE, but with different shapes and attitude: one spherical, and one cylindrical satellite. In both cases the reference orbits are generated by a simulator tool, and play the same role of the GOCE POD. To this purpose, the idea is to simulate the reference orbit with a density model, and then to test the behavior of a PWC drag coefficient estimation by using another, different, model. The differences between the two different density models have to be interpreted as errors/uncertainties with respect to the simulated reality. We already showed that the radar-based orbit determination tries to capture the average value of the PWC function, thus we believe that determining its behavior ($C_d A$ and corresponding missing acceleration) will give us significant information for the preliminary generalization test.

Also in this case, the estimation of a 30min PWC ballistic coefficient function is performed, and the final 3D-RMS difference in position with respect to the reference orbit is less than 10m.

6.1. Preliminary test with spherical object

The first object we consider has a constant ballistic coefficient. In other words, we generate the orbital motion of a sphere-like object which has an orbit very similar to GOCE.

This simulated object has a $C_d A = 3.4\mathrm{m}^2$ and a re-entry at 90km on Nov-11$\sim$00:45 UTC. We pointed out that Figures 3 and 4 represent the unknown portion of drag modeling due to atmospheric environment models and attitude motion of the spacecraft. The useful aspect of the spherical object is that we do not have uncertainties in its cross sectional area or attitude motion, hence, apart from gas-surface interactions, we can isolate the effects due to the atmospheric environment.

We can recognize in Figure 10 the same kind of oscillations of Figure 4, confirming that the short-term oscillations are most likely driven by the errors in the atmospheric density models. In this case we used Jacchia-Roberts static in the simulator, and NRLMSISE00 in the estimator.

The long-term behavior of the function exhibits much less variations with respect to the GOCE one, suggesting that it is mainly governed by the average attitude state (e.g. large yaw variations for GOCE) and physical properties of the spacecraft. Medium-term oscillations at the order of $\sim$1-day are also evident.

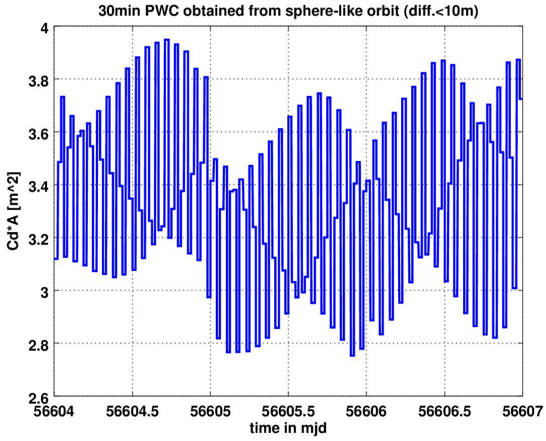

Figure 10. 30min-PWC $C_d A$ [m^2] coefficient estimation from sphere-like reference orbit (Jacchia-Roberts static vs. NRLMSISE00).

6.2. Preliminary test with cylindrical object

The second object that we analyze is a cylinder, whose orbit was generated by BRL's 6DOF propagator ATS6. This object is a cylinder with a forward center of gravity of +0.32m, which potentially gives it a favored orientation. It is propagated from the same initial conditions of GOCE on Oct-22, with analogous shape, size, and mass characteristics, but starting from an initial unstable, backward orientation. The result is a vehicle which tumbles, but aligns in the final two days (see Figure 11). The tumbling motion significantly raises the average drag leading to a shorter trajectory, and it has indeed a re-entry at 90km on Oct-28$\sim$1:50 UTC.

In this case we used the Jacchia-Roberts dynamic density model in the simulator, and the NRLMSISE00 in the estimator. We find a confirmed much larger average value of the estimated drag PWC function due to the tumbling motion, and larger (about proportional) short/medium-term oscillations (Figure 12). A significant decrease in the long-term average value is visible in the last two days, due to attitude stabilization.

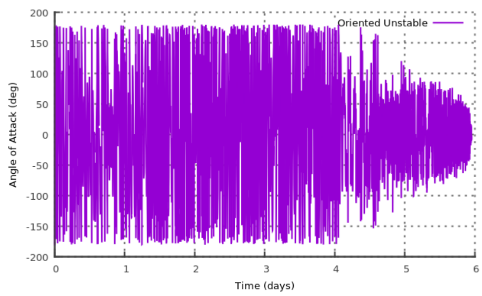

Figure 11. Angle of attack of the oriented-unstable cylinder, propagated from Oct-22 to Oct-28.

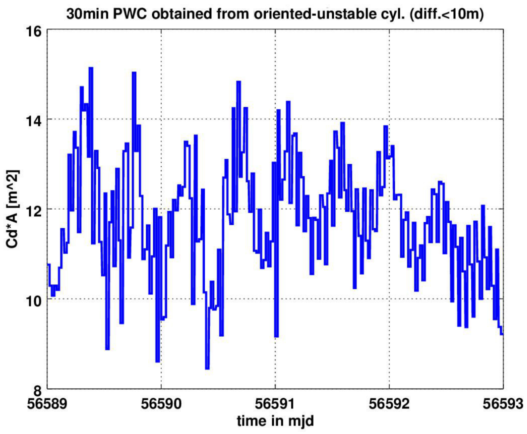

Figure 12. 30min-PWC C_dA [m^2] coefficient estimation from oriented unstable cylinder's reference orbit (Jacchia-Roberts dynamic vs. NRLMSISE00).

7. CONCLUSIONS

In this work we focused on the aspects related to the radar-based orbit determination of the GOCE spacecraft, during the last days of its decay phase, and to the corresponding ballistic coefficient estimation for re-entry predictions.

In order to perform all the necessary analysis and tests, we used the SpaceDyS's software GREOD, which is capable to perform precise orbit determiantion and parameter estimation, and to simulate orbital motion and tracking measurements.

The main analysis strategy consisted in three steps. The first one was the generation of the GOCE POD from accurate GPS measurements, and the extrapolation of a refined ballistic coefficient behavior through a PWC function estimation. The second step was the exploitation of the POD as ground-truth for the simulation of radar measurements from multiple ground stations, to calibrate the ballistic coefficient under different observational scenarios, with standard techniques. The third step was to compare the useful information that can be extracted from the large amount of GPS data, with the one extracted from sparse radar measurements, to perform re-entry predictions.

The main result is that, with a reasonable frequency of measurements, radar-based OD is very effective in estimating the average evolution of the spacecraft's ballistic coefficient, in comparison to the one estimated from GPS-based POD, even from a single site.

The high orbit accuracy provided by POD hides the intrinsic large errors in the dynamical models, atmospheric environment, and attitude behavior, which are artificially absorbed by fitted empirical accelerations. These errors re-appear in the radar-based OD under the form of large observational residuals.

Even without taking into account the uncertainties in the dynamical, and atmospheric, environment in between the current epoch of prediction and the actual re-entry, even with a very good knowledge of the initial position and velocity of the spacecraft, and with a good average drag estimation, in general it is not possible to deterministically predict the residual lifetime with very high accuracy, e.g. always much better than 10%. For this reason, to guarantee observational sessions up to few hours before re-entry is always recommended to reduce the size of re-entry windows, and this requires the use of additional ground stations especially during the last day of the decay phase.

ACKNOWLEDGMENTS

This work was carried out under ESA Contract No. 4000115172/15/F/MOS "Benchmarking re-entry prediction uncertainties". The support of the ESA Space Debris Office is gratefully acknowledged. The authors are particularly thankful to Alessandro Rossi for his precious comments and suggestions during the project.

REFERENCES

1. Bock H., Jäggi A., Beutler G., (2014). GOCE: precise orbit determination for the entire mission, *J. Geod.*, **88**, 1047–1060
2. Gini F., Otten M., Springer T., et al., (2014). Precise Orbit Determination for the GOCE Re-Entry Phase, *Proceedings of the fifth international GOCE user workshop*, ESA Publications Division, European Space Agency, Noordwijk, The Netherlands
3. Lemmens S., Bastida Virgili B., Flohrer T., et al., (2014). Calibration of Radar Based Re-entry Predictions, *Proceedings of the fifth international GOCE user workshop*, ESA Publications Division, European Space Agency, Noordwijk, The Netherlands
4. Bastida Virgili B., Flohrer T., Lemmens S., et al., (2014). GOCE Re-entry Campaign, *Proceedings of the fifth international GOCE user workshop*, ESA Publications Division, European Space Agency, Noordwijk, The Netherlands
5. Pardini C., Anselmo L., (2014). GOCE Re-Entry Predictions for the Italian Civil Protection Authorities, *Proceedings of the fifth international GOCE user workshop*, ESA Publications Division, European Space Agency, Noordwijk, The Netherlands
6. Bastida Virgili B., Flohrer T., Krag H., et al., (2012). Supporting Conjunction Event Assessments by Acquiring Tracking Data, Conference Paper IAC-12.A6.2.17
7. Jäggi. A., Beutler G., Hugentobler U., (2006). Pseudo-stochastic orbit modeling technique for low Earth orbiters, *J. Geod.*, **80**(1), 47–60
8. Montenbruck O., van Helleputte T., Kroes R., Gill E., (2005). Reduced dynamic orbit determination using

GPS code and carrier measurements, *Aerospace Science and Technology*, **9**, 261–271

9. Montenbruck O., Gill E., (2005). Satellite Orbits, Springer-Verlag Berlin Heidelberg
10. Pardini C., Anselmo L., (2001). Comparison and Accuracy Assessment of Semi-Empirical Atmosphere Models through the Orbital Decay of Spherical Satellites, *The J. of the Astr. Sci.*, **49**(2), 255–268
11. Pardini C., Anselmo L., (2008). Impact of the time span selected to calibrate the ballistic parameter on spacecraft re-entry predictions, *Adv. in Sp. R.*, **41**, 1100–1114
12. Saunders A., et al, (2012). Deriving Accurate Satellite Ballistic Coefficients from Two-Line Element Data, *J. of Spacecraft and Rockets*, **49**(1)
13. Wilkins M., Alfriend K., (2000). Characterizing orbit uncertaintiy due to atmospheric uncertainty, AIAA/AAS Astrodynamics Specialist Conference and Exhibit, Denver CO, American Institute of Aeronautics and Astronautics
14. Siminski J., (2016). Techniques for assessing space objects cataloguing performance during design of surveillance systems, 6th International Conference on Atrodynamics Tools and Techniques (ICATT), 14-17 March 2016, Darmstadt